Design and modelling of automated reactor for the production of caustic potash from cocoa pod husk.

Available online at www.sciencedirect.com

ScienceDirect

Procedia CIRP 84 (2019) 960–965

www.elsevier.com/locate/procedia

29th CIRP Design 2019 (CIRP Design 2019)

Design and Modelling of Automated Reactor for the Production of Caustic Potash from Cocoa Pod Husk

Daniyan, I. A. [a*], Mpofu, K.[a] , Daniyan, O. L.[b], Adeodu, A. O.[c], Uchegbu, I. D.[c]

[a]Department of Industrial Engineering, Tshwane University of Technology, Pretoria, South Africa.*
[b]Centre for Basic Space Science, University of Nigeria, Nsukka, Nigeria.
[c]Department of Mechanical and Mechatronics Engineering, Afe Babalola University, Ado Ekiti, Nigeria.

* Corresponding author. Tel.: +27 (064) 541-3537, *E-mail address:* afolabiilesanmi@yahoo.com

Abstract

The need for the waste to wealth conversion triggered the design and modelling of an automated reactor for the production of caustic potash from cocoa pod husk. The system, which was designed for an annual production target of 35,000 tons, comprises of seven units namely; the storage unit, fluidized bed dryer and rotary dryer, roll crusher, reactor, furnace, condenser, and evaporator. The mechanical design and modelling was carried out with the aid of the Auto desk Inventor 2017 while the ASPEN HYSYS was employed as a process modelling tool for the material, energy optimization and plant economics. The design of the system also incorporates an Arduino Uno Microcontroller to a pH, pressure and temperature sensors to monitor the process conditions of the designed reactor. Stainless steel was selected for the fabrication of the reaction because of its excellent corrosion resistance ability, strength and machinability. The results of the Finite Element Analysis (FEA) carried out indicates that the material used for the reactor development is likely to yield when loaded beyond its tensile strength. The successful completion of this work provides design data for scaling the development of KOH reactor and a framework for KOH production from the cocoa pod husk.

Peer-review under responsibility of the scientific committee of the CIRP Design Conference 2019.

Keywords: Automated reactor, caustic potash, design, KOH, modelling

1. Introduction

Some plants and residues from agricultural products are rich in alkali metals such as potassium, calcium, sodium and magnesium which when burnt in the presence of air and water vapour produces respective oxides and hydroxides [1]. Cocoa is produced in large quantities in many African countries, yet the by-product in the form of pod husk, which is rich in potassium, has not been optimally harnessed despite its prospects [2-4]. In a bid to build a sustainable and sound material-cycle society through the effective use of waste resources, agricultural residues generated from cocoa processing, can be converted from waste to wealth since it is a recyclable material [5]. Research have proven that beside the environment pollution caused by the indiscriminate disposal of the cocoa pod husk, it is also capable of depleting the soil nutrient when disposed on farmland [6-7]. There is therefore the need to convert waste to wealth through the processing of cocoa pod husk for the formulation of animal feed, catalyst [8-10] or caustic potash [11]. Proper harnessing of the cocoa pod husk will contribute significant to gross domestic product and generate employment opportunities. Also, there will be significant reduction in environmental pollution and depletion of soil fertility emanating from indiscriminate disposal while enhancing economic sustainability [12-13]. Caustic potash one of the products of cocoa pod husk leaching finds versatile industrial application [14-16]. For instance, it can be employed for the production of soap, detergent, fertilizers, pharmaceuticals and other photographic chemicals, alkaline battery. It is also a useful dehydrating agent for drying gases, as a lubricant in the extrusion pressing of melting alloys, as a cleaner for eliminating scales from the surface of titanium alloy intermediates, in descaling ferrous metals, in the refining of petroleum fractions, for metal cleaning operations, lye peeling, in removing insulating coatings from ore and in

2212-8271 © 2019 The Authors. Published by Elsevier B.V.
Peer-review under responsibility of the scientific committee of the CIRP Design Conference 2019.
10.1016/j.procir.2019.03.201

electrolytic strip bath [17-18]. Ahmad *et al.* [19] considered the production of caustic potash using solar powered diaphragm cells. The work showed the possibility of producing caustic potash in an energy efficient way compared to conventional means. Also Daniyan *et al.* [20] designed a processor for the production of caustic potash from cocoa pod husk. The material and energy balance as well as process design were sufficiently highlighted. Many works have been reported on the use of leaching technique for the production of caustic potash from cocoa pod husk as well as the optimization of process parameters for the increased yield of the product. However, the analysis of integration features of the overall process for the production of caustic potash from different feedstock has been a missing link and detail mechanical and process design issues have not been sufficiently highlighted. These are areas of interest in this research work with a view of getting a comprehensive picture of the role of mechanical, process design and engineering in the caustic potash production processes.

2. Method

2.1 Description of the leaching process

The dried cocoa pod husk are crushed to lump size and passed to the furnace operated at a temperature of about 700ºC for ashing. The ashed intermediate product is first allowed to cool and the transferred to the reactor at room temperature. Inside the reactor, the ashed intermediate products is mixed with water at a ratio of about 1:20 wt.% at a temperature of about 60ºC and the soluble solute (KOH) is leached out after about 30 minutes. The process design is shown in Fig. 1.

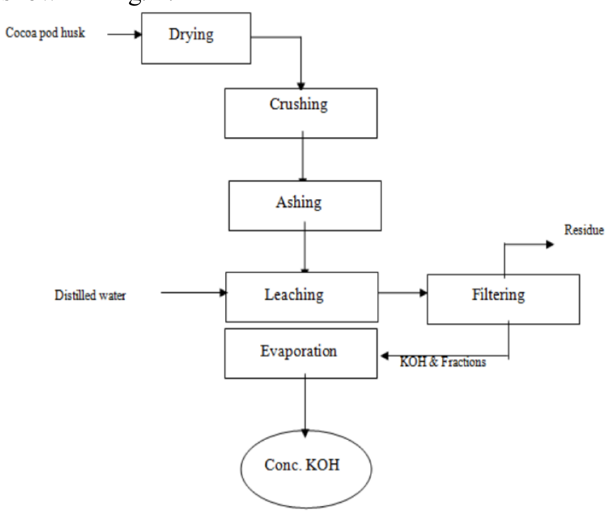

Fig. 1: Process design for KOH production [20].

The reaction kinetics of the leaching process of conversion of cocoa pod husk to caustic potash is expressed as Equation 1 to 3.

$$K_2O + CO_2 = K_2CO_3 \quad (1)$$
$$K_2CO_3 + H_2O + CO_2 = 2KHCO_3 \quad (2)$$
$$K_2CO_3 + H_2O += KOH + KHCO_3 \quad (3)$$
$$k_1 = 2.0 \times 10^{60}, k_2 = 2.07, k_3 = 0.99$$

The chemical composition of the cocoa pod husk is presented in Table 1.

Table 1: Chemical composition of the cocoa pod husk

S/N	Constituents of Cocoa pod husk	% composition of constituents
1.	Water	57.75
2.	Total dry matter	42.25
	Total	100
1.	Crude protein	8.69
2.	Pure protein	-
3.	Fatty substance	0.15
4.	Ash (SIO free)	10.80
5	Crude fibre	33.90
6.	Nitrogen free extracts	41.21
7.	Glucose	1.16
8.	Sucrose	0.18
9.	Pectin	3.71
10	Theobromine	0.20

Source: [20]

2.1 Process design

Targeted output is 35,000 tons per anum (35,000,000 kg)
Calculated input of fresh cocoa pod husk is 3,750,000 tons (3,750,000,000 kg)
The reactor unit
This unit is employed basically for leaching the KOH (Fig. 2)

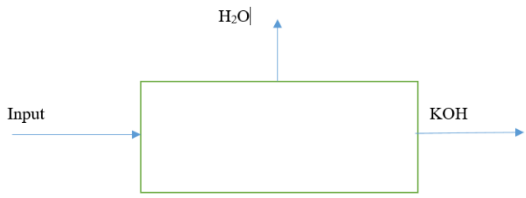

Fig. 2: The reactor unit

The input to the reactor are as follow;
K_2O: 74.42%, MgO: 9.44%, CaO: 5.74%, P_2O_5: 6.83%, SiO_2: 1.57%, Others: 2%

$$K_2O + H_2O \rightarrow 2KOH$$
$$MgO + H_2O \rightarrow Mg(OH)_2$$
$$CaO + H_2O \rightarrow Ca(OH)_2$$

Mass of K_2O in ash= $0.7442 \times 61{,}842{,}919 = 46{,}023{,}500.3\ kg$

Molar mass of K_2O= 71

Amount of K_2O= $\frac{46{,}023{,}500.3}{71} = 648{,}218.314\ kmol$

$$1\ kmol\ of\ H_2O = 2\ kmol\ of\ KOH$$
$$648{,}218.314 = x$$
$$kmol\ of\ KOH = 1{,}296{,}436.63\ kmol$$

Since molar mass of KOH is 56 g/mol.

$$kmol\ in\ masss = 1{,}296{,}436.63 \times 56$$
$$= 7{,}2600{,}451.3\ kg\ (KOH\ solution)$$

Amount of H_2O reacted=648218.314 kmol. (From the stoichiometric equation)

$$mass\ of\ H_2O = 648{,}218.314 \times 18 = 11{,}667{,}929.7\ kg$$

Product specification (10% H_2O, 90% KOH)
Production rate is annual 35,000,000 kg; monthly 3,000,000 kg; daily 100,000 kg and hourly 4166.666 kg/hr. The production stages of the KOH is shown in Fig. 3.

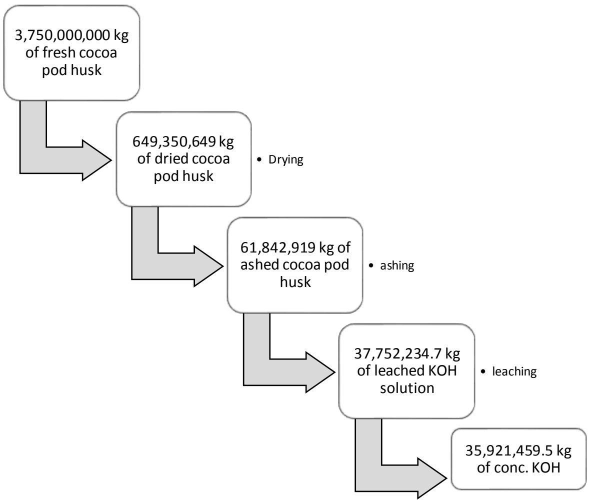

Fig. 3: The production stages of KOH

The energy balance in the reactor is given as

1. $K_2O = 74.42\%$, $C_p = 83.62\, J/mol.K$
$$Q = mC_p\Delta T$$
$$Q = 648218.314 \times 83.62 \times 358 = 1.940 \times 10^{10}\, KJ$$
2. $MgO = 9.44\%$, $C_p = 37.8\, J/mol.K$
$$Q = mC_p\Delta T$$
$$\frac{0.0944 \times 61842919}{40.3044} = 14484700.31\, kmol$$
$$Q = 144847.003 \times 37.8 \times 358 = 1.96 \times 10^9\, KJ$$
3. $CaO = 5.74\%$, $C_p = 44.29\, J/mol.K$
$$\frac{0.0574 \times 61842919}{56.0774} = 63301.500\, kmol$$
$$Q = mC_p\Delta T$$
$$Q = 63301.5 \times 44.29 \times 358 = 7.9156 \times 10^4\, KJ$$
4. $P_2O_5 = 6.83\%$, $C_p = 37.8\, J/mol.K$
$$\frac{0.06843 \times 61842919}{283.89} = 14878.5493\, kmol$$
$$Q = mC_p\Delta T$$
$$Q = 144847.003 \times 37.8 \times 358 = 1.96 \times 10^9\, KJ$$
5. $S_iO_2 = 1.57\%$, $C_p = 690\, J/mol.K$
$$\frac{0.0157 \times 61842919}{60.08} = 16160.68\, kmol$$
$$Q = mC_p\Delta T$$
$$Q = 16160.68 \times 690 \times 358 = 3.992 \times 10^9\, KJ$$
Others

6. $KHNO_3 = 1.55\%$, $C_p = 95.06\, J/mol.K$
$$\frac{0.00155 \times 61842919}{102.1111} = 938.747\, kmol$$
$$Q = mC_p\Delta T$$
$$Q = 938.747 \times 95.06 \times 358 = 3.194 \times 10^7\, KJ$$
7. $NH_4NO_3 = 0.252\%$, $C_p = 4184\, J/mol.K$
$$\frac{0.00252 \times 61842919}{80.05} = 1946.835\, kmol$$
$$Q = mC_p\Delta T$$
$$Q = 1946.835 \times 4148 \times 358 = 2.916 \times 10^9\, KJ$$
8. $NaOH = 0.660\%$, $C_p = 28.230\, J/mol.K$
$$\frac{0.00660 \times 61842919}{39.997} = 10204.847\, kmol$$
$$Q = mC_p\Delta T$$
$$Q = 10204.847 \times 28.230 \times 358 = 1.031 \times 10^8\, KJ$$
9. $Ca(OH)_2 = 0.421\%$, $C_p = 1.2142\, J/mol.K$
$$\frac{0.00421 \times 61842919}{74.093} = 3513.944\, kmol$$
$$Q = mC_p\Delta T$$
$$Q = 3513.944 \times\times 1.2142 \times 358 = 1.527 \times 10^6\, KJ$$
10. $Al(OH)_3 = 0.512\%$, $C_p = 1.4821\, J/mol.K$
$$\frac{0.00521 \times 61842919}{78.0036} = 4059.245\, kmol$$
$$Q = mC_p\Delta T$$
$$Q = 4059.245 \times 1.4821 \times 358 = 2.153 \times 10^6\, KJ$$

$$E = (1.94 \times 10^{10} + 1.96 \times 10^9 + 7.9156 \times 10^4 6.435 \times 10^8 + 3.99 \times 10^9 + 1.23 \times 10^6 + 3.194 \times 10^7 + 2.90 \times 10^9 + 1.031 \times 10^8 + 1.527 \times 10^6 + 2.153 \times 10^6)$$

$E = 2.9038 \times 10^{10}\, kJ$ (Total energy balance in the reactor)

2.2 Mechanical design

In order to meet the expected output and production rates, the volume of the reaction tank (cylinder) is calculated as 10 m^3 using Equation 4

$$V = \pi r^2 h \tag{4}$$

Where

V is the tank volume (m^3), h is the height of the tank (m) and r is the radius of the tank (m)

The thickness t of the cylindrical tank is 15 mm calculated from Equation 5.

$$t = \frac{pd}{2\sigma_c \eta} \tag{5}$$

where:

p is the internal pressure, (N/mm^2), d is the diameter of the tank, (mm), σ_c is the circumferential stress, (N/mm^2) and η is the efficiency of joint.

The shaft design consists of the determination of the correct shaft diameter that will ensure satisfactory rigidity and strength when the shaft transmits power under different operating and loading conditions [21]. For shaft with keyway (stainless steel), the allowable shear stress is given as 55 MN/m^2 [22].

The total torque required to overcome the viscosity and shear through the mixture is given by Equation 6.

$$T = \frac{P}{2\pi N} \tag{6}$$

where:

P is the power of the electric motor, (watts); and N is the number of revolution per sec

The shaft is solid with a diameter of 40 mm. The formula used for determining the diameter of a shaft having little or no axial loading according to Hall *et al.* [22] is given in

Equation 7.

$$d^3 = \frac{16}{\pi S_s}\sqrt{(K_b M_b)^2 + (K_t M_t)^2} \quad (7)$$

where:

M_t is the torsional moment, (Nm), M_b is the bending moment, (Nm), K_b is the combined shock and fatigue factor applied to bending moment, K_t is the combined shock and fatigue factor applied to torsional moment, S_S is the allowable shear stress, (N/m^2) and d is the shaft diameter, (m).

The energy required to heat the mixture of ash and water from ambient temperature of 25℃ to 60℃ is heat transferred to the fluid (work done by the heater) is given by Equation 8.

$$Q = mCp\Delta T \quad (8)$$

where:

m is the mass of stream (kg), Cp is the specific heat capacity of the stream (kJ/kgK); and ΔT is the temperature difference, (℃)

According to Rajput [23], the rating for heater is given by Equation 9.

$$P = \left(\frac{Q}{t}\right) \quad (9)$$

where:

Q is the quantity of heat supplied, (Joules) and t is the time taken to make such supply, (sec). The CAD design of the solid works is shown in Fig. 4.

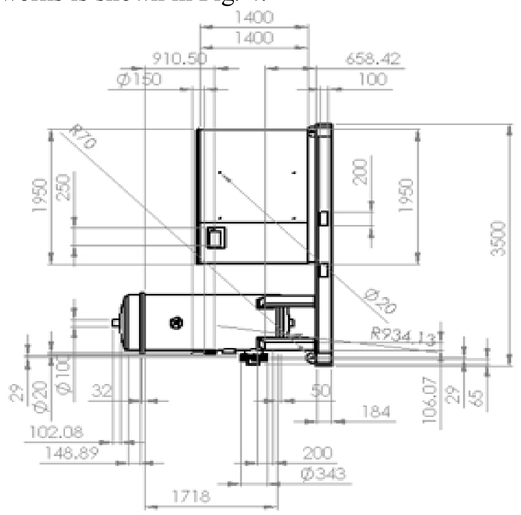

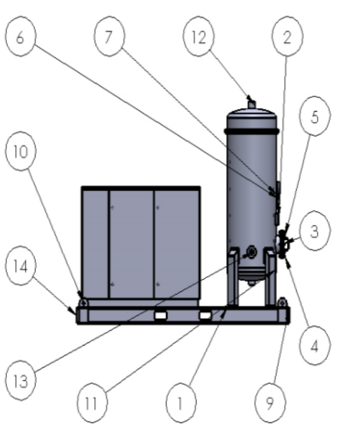

Item no	Description	Qty
1.	Shell	1
2.	Pad	1
3.	Outlet	1
4.	Bolt 8	8
5.	Nut 8	16
6.	Flange	1
7.	Pressure gauge	1
8.	Pressure gauge pointer	1
9.	Base	1
10.	Compressor	1
11	Leg support	3
12	Inlet cover	1
13	Manhole 8	1
14.	Base plate	1

Fig. 4: CAD of the reactor

Stainless steel material type was selected for the fabrication of the reactor. This is because of its high resistance to corrosion, good weldability and formability as well as high strength under loading. The mechanical and thermal properties of the stainless steel material is presented in Table 2.

Table 2: Mechanical and thermal properties of the stainless steel

	Mechanical	
S/N	Property	Value
1.	Density	7300 kg/m^3
2.	Brinell's hardness	123
3.	Ultimate tensile strength	448 MPa
4.	Yield strength	241 MPa
5.	Modulus of Elasticity	190 GPa
6.	Poisson's ratio	0.26
7.	Shear modulus	78 GPa
	Thermal	
8.	Specific heat capacity	0.5 kJ/kgK
9.	Thermal conductivity	162 W/m.K
10.	Thermal expansion coefficient	1.5E-05 K^{-1}
11.	Melting Point	1450^{o}C

A 220 V power supply is used to power the heater while a temperature probe connected to the heating element is used to measure and monitor the temperature. The readings from the probe is amplified and sent to the micro controller (8-bit Atmel ATmega328p) for control action. If the measured value exceeds the threshold, value pre-set on the controller, the heating element will automatically trip off. On the other hand, the heater will be activated via a contactor when the measured value is less than the threshold.

The probe is made of stainless steel material and has a temperature range of -40℃ to 380℃ and length of 500 mm, diameter 5 mm (Fig.4).

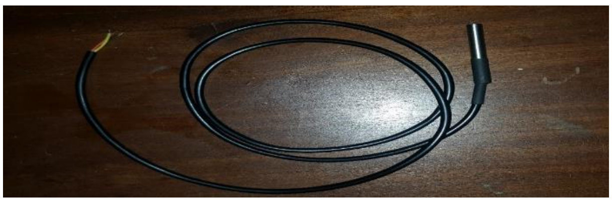

Fig. 5: Temperature probe

The circuit diagram is shown in Fig. 6

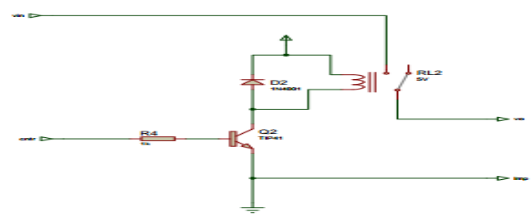

Fig. 6: Circuit diagram for the heating element

A pressure sensor with a working pressure range of 0-1.2

MPa is also incorporated to measure the pressure of the system and converts measured values into voltage (Figure 7).

Figure 7: Pressure transducer sensor

The main controller is the Arduino microcontroller board, which uses the microchip ATmega 328p microcontroller for control action (Fig. 8). It comprises of 14 digital pins with 6 analog input and output pins which is programmable with the Arduino Integrated Development Environment (IDE). The thresholds values of the process variables such as temperature and pressure are pre-set on the micro controller and the measured values are compared with the threshold for correction of any deviation or error generated

Fig. 8: Arduino microcontroller board

Table 3 shows the technical features of the Arduino microcontroller.

Table 3: Technical specifications of the Arduino micro controller

S/N	Item	Value
1	Micro-controller	8-bit Atmel ATmega328p
2	Operational voltage	5V
3	Digital GPIO	14
4	Analog IO	6
5	Program memory	Flash 32kb, EEPROM 1kb
6	Clock speed	16MHz
7	USB	Type B socket
8	Programmer	In-system firmware
9	Serial communications	SPI, I2C

3. Results and Discussion

Fig. 9-11 show the Finite Element Analysis carried out using solid works. The Von Mises stress analysis is a function of the maximum distortion energy. Hence, from Fig. 4, the minimum and maximum values of the stress under loading are 8.252 N/m^2 and 320 MN/m^2. Since the yield strength of the material, which is an indication of the point at which the material deforms upon loading, is 241 MN/m^2, it then implies that the material of the reactor will yield to deformation at stresses above 241 MN/m^2.

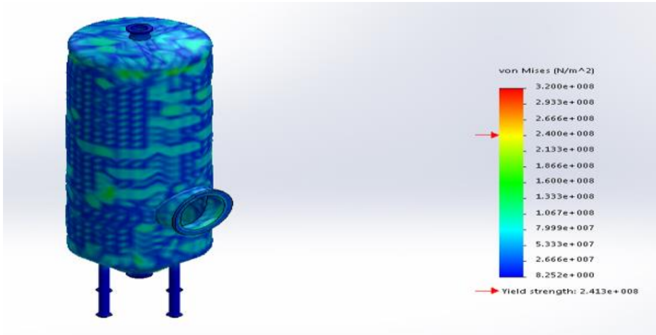

Fig. 9: Stress distribution analysis of the reactor

Fig. 10 shows the displacement analysis of the reactor due to loading. The value of the miimum and maximum displacement was 1. 000E-30 mm and 1.619 mm respectively. The dispcement was observed to increase with increase in loading causing stress to build up within the material. Below the yield point, the value of displacement was insignificant. The increase in loading beyond the yield point of the material causes significant displacement which can cause vibration and noise.

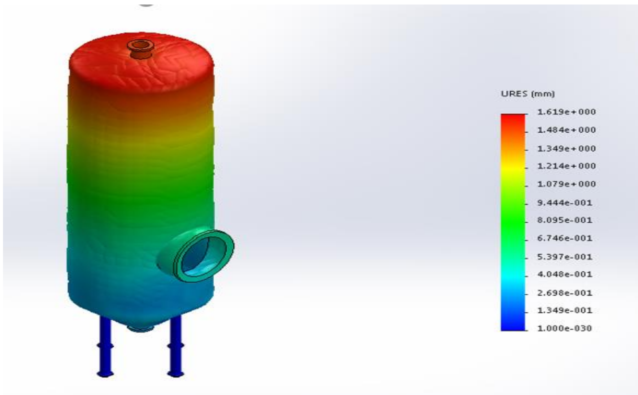

Fig. 10: Displacement analysis of the reactor

Fig. 11 shows the strain distribution analysis of the reactor. The strain is the measure of the plastic deformation due in the direction of the applied force with respect to the initial dimension of the material. The minimum and maximum value obtained was 3.18E-11 and 1.03 E-003 respectively. The strain increases when the material is loaded beyond the yield strength.

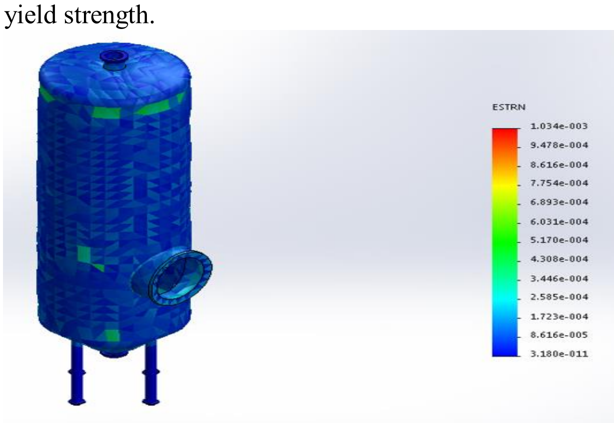

Fig. 11: Stain distribution analysis of the reactor

4. Conclusion

The design and optimization of an automated reactor for the production of caustic potash from cocoa pod husk was carried out. The Auto desk Inventor 2017 was employed as a design, modelling and finite element analysis of the reactor while the Arduino micro controller was employed for control actions. The Finite Element Analysis carried out indicates that the material used for the reactor development is likely to yield when loaded beyond its tensile strength. The successful completion of this work provides design data for scaling the development of KOH reactor. This work finds application in the process and manufacturing industries as it provides detailed analysis of the mechanical, process design and automation of the KOH reactor. Future work can consider the scaling of the reactor's specifications for fabrication based on design requirements.

References

[1] Kumar, A. Extraction of caustic potash from coffee husk: process optimization through response surface methodology, Int. J. Chem. Sci.: 11(3):1261-1269, 2013.

[2] Zawawi, D., Angzzas, S. M. K., Ashuvila, M. A., Halizah, A., Hatta, M. Z. M. Chemical composition and morphological of cocoa pod husks and cassava peels for pulp and paper production. *Australian Journal of Basic and Applied Sciences,* 7(9): 406-411, 2013

[3] Babayemi, J. O., Adewuyi, G. O., Dauda, K. T. and A. A. Kayode. The ancient alkali production technology and the modern improvement. A Review*: Asian Journal of Applied Sciences*. 4:22-29, 2010.

[4] Babayemi, J.O., Dauda, K. T., Nwude, D. O. and Kayode, A. A. Evaluation of the composition and chemistry of ash and potash from various plant materials. A Review*: Journal of Applied Sciences* 10: 1820-1824, 2010.

[5] Babayemi, J. O. and Adewuyi, G. O. Assessment of combustion and potash production as options for management of wood waste. *Journal of Applied Sciences and Environmental Management.* 14(1):73-75, 2010.

[6] Ogundiran, M. B., Babayemi, J. O. and Nzeribe, C. G. Cashew nut shell as source of ash for potash production. *Bioresource Technology*, 6(1):529-536, 2011

[7] Akunna, T. O., Ahaotu, E. O. Osuji, C. N. and Ibeh, C. C. Production of soap using palm bunch ash. International Journal of *Applied Sciences and Engineering*, 1(2):79-82, 2013.

[8] Isika, M.A., Nsa, E. E. and Ozung, P. O. Replacement value of processed cocoa bean meal for groundnut cake in rations for fryer rabbits. *J. Sustain. Technol.,* 3(1): 118-127, 2012.

[9] Khanahmadi, S., Yusof, F., Ong, H. C., Amid, A., and Shah. Cocoa pod husk: A new source of CLEA-lipase for preparation of low-cost biodiesel: An optimized process *Journal of Biotechnology*, 231:95-105, 2016.

[10] Oddoye, E. O. K., Rhule, S. W. A. Agyente-Badu, K., Anchirinah, V. and Owusu Ansah, F. Fresh Cocoa pod husk as an ingredient in the diets of growing pigs. Sci. Res. Essays, 5(10): 1141-1144, 2010.

[11] Olufemi, A. S., Olayebi, O. O. and Makpah, D. E. A novel process for the production of potash from plant ash: leaching technique. *Journal of Advancement in Engineering and Technology,* 5(1):1-5, 2017.

[12] Olufemi, A. S., Azeez, M. A. and Olayebi, O. O. Process intensification of colemanite leaching using sulfuric acid in a batch reactor. *International Journal of Engineering Research and General Science,* 4(4):149-160, 2016.

[13] Napo, D., Ntuli, F. Muzenda, E. and Mollagee, M. Process intensification of zinc oxide leaching process using sulphuric acid," in Proceedings of the World Congress on Engineering and Computer Science, 2011 Vol II WCECS 2011, October 19-21, 2011, San Francisco, USA.

[14] Cruz, G., Pirilä, M., Huuhtanen, M., Carrión, L., Alvarenga, E. and Keiski, R. L. Production of activated carbon from cocoa (Theobroma cacao) pod husk. *Journal Civil and Environmental Engineering,* 2(2): 1-

[15] Akpakpan, A.E., Akpabio, U. D., Ogunsile, B. O. and Eduok, U. M. Influence of cooking variables on the soda and soda-ethanol pulping of Nypa Fruticans Petioles. *Australian Journal of Basic and Applied Sciences,* 5(12): 1202-1208, 2011.

[16] Ozung, P. O. Kennedy Oko, O. O. and Agiang, E. A. Chemical composition of differently treated forms of Cocoa Pod Husk Meal (CPHM). *Asian Journal of Agricultural Sciences*, 8(2): 5-9, 2016.

[17] Adamafio, N.A., Ayombil, F. and Tano-Debrah, K. Microbial detheobromination of cocoa (Theobroma cacao) pod husk. *Asian J. Biochem.,* 6(2): 200-207, 2011.

[18] Marques, G., Rencoret, J., Ana, G., and José, C. D. R. Evaluation of the chemical composition of different non-woody plants fibers used for pulp and paper manufacturing. *The Open Agriculture Journal,* 4:93-101.

[19] Ahmad, W. A. O. and Abdelmaged, A. Production of caustic soda using solar powered diaphragm cells. *IOSR Journal of Applied Chemistry,* 8(2): 09-16, 2015.

[20] Daniyan, I. A., Adeodu, A. O. and Adewumi, D. F. Design of a processor for the production of 30,000 tons of caustic potash per anum from cocoa pod husk. *International Journal of Science and Research,* 3(3):691-700, 2014.

[21] Ashby, M., Shercliff, H. and Cebon, D. Materials Engineering, Science, Processing and Design. Rajkamal Press, India: 21-31, 2007.

[22] Hall, A. S., Holowenko, A. R. and Laughlin, H. G. Machine Design. Purdue University Press: 113-130, 1980.

[23] Rajput, R. K. Fluid Mechanics. Chand Publishing Limited. pp. 132-204, 2008.

This is a resupply of March 2023 as the template used in the publication of the original article contained errors. The content of the article has remained unaffected.